Journal of Hazardous Materials 176 (2010) 154–164

Contents lists available at ScienceDirect

Journal of Hazardous Materials

journal homepage: www.elsevier.com/locate/jhazmat

Electrochemical degradation of specialty chemical industry effluent

C. Ahmed Basha [a,*], P.A. Soloman [b], M. Velan [b], Lima Rose Miranda [b], N. Balasubramanian [b], R. Siva [b]

[a] Central Electrochemical Research Institute (CSIR), Karaikudi 630 006, Tamilnadu, India
[b] Department of Chemical Engineering, A.C. Tech Campus, Anna University-Chennai, Chennai 600 025, India

ARTICLE INFO

Article history:
Received 22 August 2009
Received in revised form 24 October 2009
Accepted 31 October 2009
Available online 10 November 2009

Keywords:
Electrochemical
Specialty chemical industry
Wastewater
Artificial neural network
Recycle reactor

ABSTRACT

Conventional wastewater treatment techniques are inefficient to manage large quantities of refractory organics discharged by specialty chemical industries. It is aimed in the present investigation to compare overall performance of the basic electrochemical reactor configurations such as batch, batch recirculation and continuous recycle reactors, in removing the organic part of wastewater from a medium-scale, specialty chemical industry. The effects of current density, supporting electrolyte concentration, electrolysis duration and fluid flow rate on the pollutant removal and energy consumption performances were critically evaluated. Continuous recycle reactor is found to be the better configuration, because of its flexibility of operation. Circulation flow rate and withdrawal flow rate enable control on transfer coefficients and treatment duration respectively. The ability of artificial neural network (ANN) in predicting the performance of the batch electrochemical treatment has also been demonstrated.

1. Introduction

Treatment and safe disposal of bio-refractory pollutants in an environmentally acceptable manner is a topic of universal importance. Speciality chemical industries require large volumes of water of high purity and discharge large quantities wastewater containing number of refractory organics pollutants. The wastewater is complex and highly variable with respect to its nature, containing high levels of chemical oxygen demand (COD around 48,000 mg L^{-1}), dissolved solids, a low level of biochemical oxygen demand, a considerable amount of total organic halogen and intense color. The most extensively applied biological treatment often fail due to the fact that many organic substances produced by the chemical and related industries are inhibitory, toxic or resistant to biological treatment. Feasibility of the various advanced oxidation processes based on ozone [1], hydrogen peroxide [2], hydrogen peroxide/ferrous ion catalyst (the so called Fenton's reagent) [3], UV radiation [4], sonochemical [5], and their combinations such as ozone/UV [6], Fenton/UV [7], ozone/UV/hydrogen peroxide [8] etc., for handling such pollutants are under investigation and their application in large scale operation in still questionable.

Various electrochemical treatments such as electrocoagulation, electro-oxidation etc. has also been studied for handing these class of pollutants [9,10]. The performance comparison of the various electrochemical techniques and advanced oxidation processes is of utmost interest of many researchers [11–13]. Electrochemical techniques have been receiving greater attention in recent years due to their distinctive advantages such as, *environmental compatibility*; (the main reactant is the electron which is a clean reagent) and *versatility* (a plethora of reactors and electrode materials, shapes, and configurations can be utilized). It is noteworthy that the same reactor can be used frequently for different electrochemical reactions with only minor changes and also the electrolytic processes can be scaled easily from the laboratory to the plant, allowing treatment volumes ranging from milliliters to millions of liters. Electrochemical methods are generally safe because of the mild conditions and innocuous nature of the chemicals usually employed. Electrodes and cells can be designed to minimize power losses due to poor current distribution and voltage drops and making the processes more competitive in energy consumption than the conventional techniques [14].

Development of phenomenological or empirical/semi-empirical equations is always time consuming and usually has low accuracy in prediction. In this context, soft computing technique like artificial neural network (ANN) provides an efficient alternative. ANN has become increasingly recommended for applications where the mechanistic description of the interdependence between variables is either unknown or very complex. One of the characteristics of modeling based on ANN is that it does not require the mathematical description of the phenomena involved in the process, and might therefore prove useful in simulating and up-scaling complex electrochemical systems. The fundamental element of ANN is the processing elements called neurons. ANN can learn the latent

* Corresponding author at: Central Electrochemical Research Institute (CSIR), Pollution Control Division, CECEI Nagar, Karaikudi 630 006, Tamilnadu, India.
Tel.: +91 4565 227550; fax: +91 4565 227713.
E-mail addresses: cab_50@rediffmail.com, basha@cecri.res.in (C. Ahmed Basha).

0304-3894/$ – see front matter © 2009 Elsevier B.V. All rights reserved.
doi:10.1016/j.jhazmat.2009.10.131

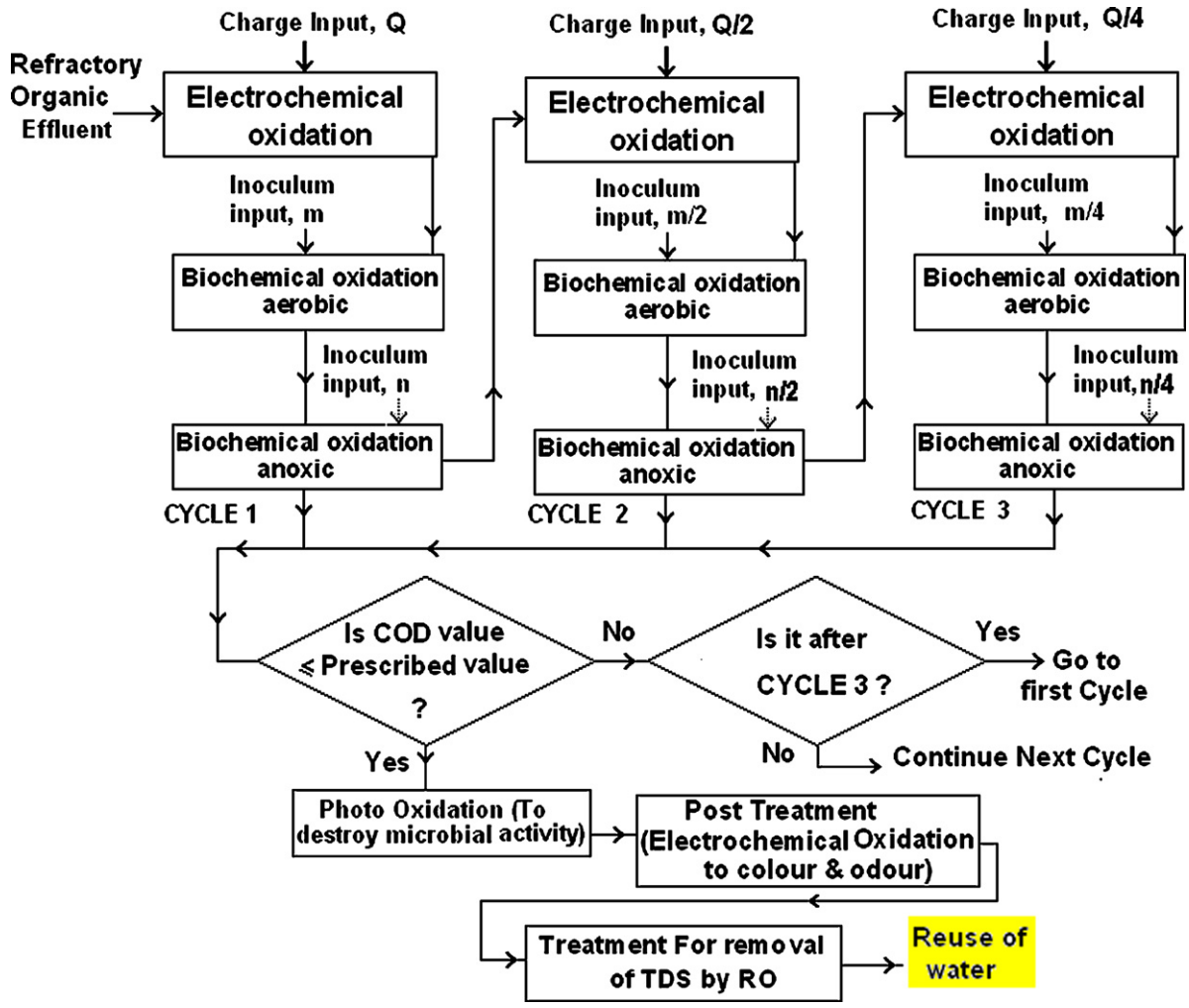

Fig. 1. The logical flow chart illustrating the technique of integrating electro-oxidation (for improvement of biodegradability) with conventional techniques such as biological treatment for complete mineralization.

relationships between the inputs and outputs without prior knowledge about functional relationship between them. ANN is more effective in expressing the non-linear relationships between the dependent and the independent variables. In addition to these, the elasticity of ANN enables updating the network with new data. The processing style of neural network is parallel and there is no strict rule or algorithm to follow. Further, ANNs are known as universal function approximators and they try to provide a tool that both programs learn on their own. Provision of model free solutions, data error tolerance, built in dynamism and lack of any exogenous input requirement makes ANN attractive [15].

In the present investigation electrochemical degradation methodology has been applied in a batch, batch recirculation and continuous recycle modes in managing the wastewater discharged by a typical medium-scale speciality chemical industry. The purpose behind the investigation is not to treat the effluent in the methodology recommended, but to estimate the energy demanded by such a treatment so that a protocol similar to the logical flow chart illustrated in Fig. 1 can be devised with the knowledge of specific energy/charge required for complete mineralization of this heavily loaded effluent (this may not be economically viable if electrochemical degradation methodology alone followed because of the energy consumption). The alternative technique is integrating the electrochemical degradation (for improvement of biodegradability [9]) with conventional techniques such as biological treatment might be well accepted. The potential of ANN in predicting the performance of the batch electrochemical treatment has also been demonstrated. It is possible to predict the extent of removal of COD by feeding the factors such as current density, time and supporting electrolyte concentration. This is useful in design and scale-up of the process.

2. Materials and methods

The effluent was collected from M/s Sanmar Speciality Chemicals Limited, Berigai, Hosur, Tamilnadu, India. This medium-scale unit manufactures performance chemicals for flavours and fragrances, resins, polymers, elastomers and intermediates for complex phytochemicals extracted from plants such as aloe vera, sunflower etc. The unit generates effluent around 35,000 L per day containing industrial solvents such as benzene, ethylbenzene, toluene, xylene and hexane and sodium chloride (used for cleaning the equipments and the processing units). Physicochemical characterization of the effluent was carried out. The effluent was found dark brown colored and almost neutral (pH 7.3). Major portion of the solids were appeared in suspension, 6300 mg L^{-1} (dissolved solids: 156 mg L^{-1}) and found heavily loaded organic matter especially in dissolved form (COD: 48,000 mg L^{-1}). The low value of its BOD_5 (1100 mg L^{-1}, biodegradability index: 0.023) indicates the inappropriateness of the conventional biological treatment.

The effluent was distilled at atmospheric pressure in a simple distillation set-up in order to measure the contribution of volatile part in the pollution load (being the case of removal of volatile part, this operation can be practiced in a solar evaporation set-up). The COD of distillate was measured 17,750 mg L^{-1} with a distillate–residue weight ratio of 4. BOD_5 of the distillate is found almost zero. The semi-solid appeared residue, after removal of the crystallised salt, was so concentrated in organic matter that it can be burned with the starting support of fuel. The electrochemical degradation of the distillate is examined in the present investigation. All the chemicals used in the study were of analytical reagent (AR) grade. COD of the samples was determined using the dichromatic open reflux method, strictly following the APHA [16]. Experiments were repeated until the difference found less than 3%. Electrochemical experiments were carried out using Ti/RuO_x–TiO_x coated titanium substrate insoluble anode (TSIA) [17] and stainless steel cathode.

2.1. Treatment in batch mode

Experimental set-up of the batch reactor used for electrochemical degradation studies consists of a Perspex cylinder of 500 mL capacity (diameter: 8 cm, height: 11 cm) with a PVC lid having the provision to fit a pair of electrodes. Provisions were also made in the lid for periodic sampling. A rectangular, stainless steel flat plate and a rectangular flat expanded mesh of titanium (catalytic oxide coated) of dimensions 5.5 cm × 6.5 cm, were functioned as the cathode and the anode respectively. The plates were arranged parallel to each other with an inter-electrode gap of 10 mm. The void fraction of the mesh type anode was 20% by area, which resulted in an effective area of 25.52 cm^2 (dipped area: 5.5 cm × 5.8 cm). The electrodes were connected to a 5 A, 10 V DC regulated power supply, through an ammeter and a voltmeter. The preliminary batch experiments on COD removal were conducted to find the influencing parameters and their experimental domain. The wastewater was prepared for improvement of its ionic conductivity by adding the required amount of sodium chloride. Since the pH of the effluent was found to be less in influencing the response (comparatively better at neutral) during the preliminary runs, no adjustment was done. The electrode plates were cleaned manually by washing them in distilled water prior to every run. The electrodes were placed in the required volume (200 mL) of wastewater taken in the cell such a way that 25.52 cm^2 of active surface of the anode immersed. The solution was constantly stirred at 200 rpm using a magnetic stirrer in order to maintain uniform concentration. DC power supply was given to the electrodes according to the required current density and the experiments were carried out under constant current conditions. The efficiency of the batch electrochemical reactor in removing the organic part of the effluent (measured through COD) was studied at various conditions of current density (up to 5.0 A dm^{-2}), supporting electrolyte concentration (up to 6 g L^{-1}) and electrolysis duration (up to 10 h). Separate experiments were conducted for the development of ANN model. Totally, 125 data were collected in random combination of factors within the experimental domain (current density: 2–7 A dm^{-2}; electrolysis time: 2–10 h; and supporting electrolyte concentration: 2–7 g L^{-1}).

2.2. Treatment in batch recirculation mode

The experimental set-up of batch recirculation/recycle mode of operation used for the electrochemical degradation studies is schematically represented in Fig. 2. By adjusting of the valves the same set-up can be operated either in batch recirculation or recycle modes (i.e., for batch recirculation mode of operation, streams 10 and 12 will be in closed condition). The electrochemical reactor is of filter press type of 700 mL capacity. Two stainless steel

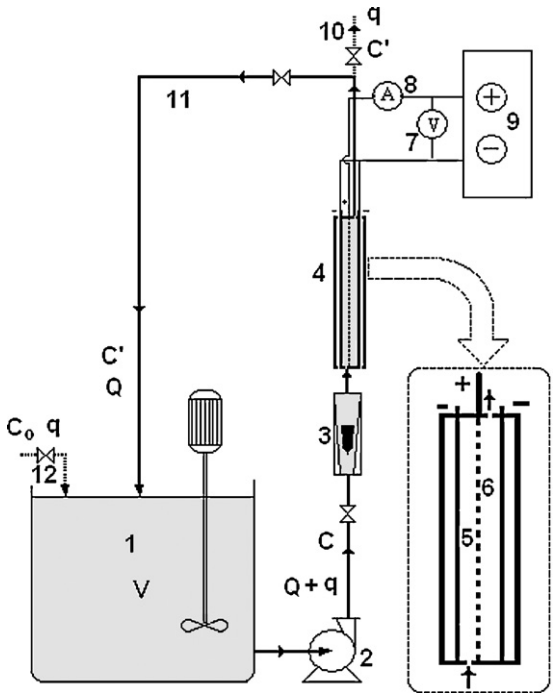

Fig. 2. Experimental set-up of flow reactor: (1) reservoir, (2) pump, (3) rotameter, (4) flow cell, (5) anode, (6) cathode, (7) digital voltmeter, (8) digital ammeter, (9) D.C. regulated power supply, (10) treated wastewater outlet, (11) recirculation stream, (12) wastewater inlet reactor, and (13) mechanical agitator. For batch recirculation system streams 10 and 12 will be absent.

rectangular flat plates and one rectangular flat expanded mesh of Ti/RuO_x–TiO_x coated titanium substrate insoluble anode (TSIA) were functioned as cathodes and anode respectively (see Fig. 2). The plates were arranged parallel to each other with a constant inter-electrode gap of 12 mm, anode being at the centre. The void fraction of the mesh type anode accounts 20% by area, which resulted in an effective anode area of 290 cm^2 (25 cm × 14.5 cm). Electrodes were connected to a 10 A, 25 V DC regulated power supply in mono-polar mode, through an ammeter and a voltmeter. The other components of the set-up being a reservoir of 5.0 L capacity, a magnetically driven self-priming centrifugal pump and a rotameter, connected using silicone rubber tubes.

The batch effluent volume considered for every experimental run was 2.0 L adjusted with supporting electrolyte concentration (5 g L^{-1}). Required flow rate through the reactor was established by pumping and adjusting the valves. The effluent enters the cell through a bottom connection provided at the gap between the anode and one of the cathode, passes through the perforations in the anode mesh plate to reach the other chamber and leaves through the outlet connection situated at the top position of the chamber. The flow rate of the effluent was measured by using a calibrated rotameter. After reaching the steady-state flow, DC power supply was given to the electrodes keeping constant current at the required level and for the set duration of electrolysis. Samples were collected from the reservoir for estimation of COD. Experiments were conducted for the cases of circulation flow rates varying from 20 to 100 L h^{-1} for two current densities of 4 and 5 A dm^{-2}.

2.3. Treatment in recycle mode

The experimental set-up of the recycle mode of operation is schematically represented in Fig. 2. Wastewater dissolved with 5 g L^{-1} sodium chloride was filled in the reservoir. The required recycle flow rate (Q) and withdrawal flow rate (q) was established by pumping and adjusting the valves. The wastewater inlet flow

rate was adjusted to reach steady state reservoir level. Keeping the recycle flow rate (Q) constant 20 L h^{-1} the inlet/discharge flow rate (q) was varied (1–6 L h^{-1}). DC power supply was connected to the electrodes keeping a constant current for the required current density of 4 A dm^{-2}. Samples were collected from the exit stream for each experimental condition for estimation of COD.

2.4. Artificial neural network

Most applications require networks that contain at least three normal types of layers—input, hidden and the output. The number of the layers and processing elements in the layers vary from one process to another. The user must determine the optimal number of layers and neurons. Generally, the number of layers and processing elements are defined by trial and error. Back-propagation method is a first order gradient method of ANN. The training of back-propagation neural network consists of two phases: a forward pass during which the processing of information occurs from the input layer to output and a backward pass when the error from the output layer is propagated back to the input layer and the interconnections are modified [18].

In the present study, feed-forward ANN model is designed in back-propagation training algorithm using the Neural Network Toolbox of MATLAB 7. The number of neurons in input and output layers depends on independent and dependent variables, respectively. Since one dependent variable—percentage removal of COD; depend on three variables—current density, electrolysis duration and supporting electrolyte concentration; one and three neurons were devoted to output and input layers respectively. All inputs and outputs were linearly normalized before entering in ANN, using the following equation [19]:

$$A_i = \frac{X_i - X_{\min}}{X_{\max} - X_{\min}}(r_{\max} - r_{\min}) + r_{\min} \quad (1)$$

where X_i is input or output of the network, A_i is the normalized value of X_i, $X_{\min}$ and $X_{\max}$ are extreme values of X_i, and $r_{\min}$ and $r_{\max}$ define the limits of the range where X_i is scaled. In this work, input and output data are normalized between −1 and 1; and 0.2 and 0.8 respectively. After modeling, results were converted to original state.

Neural Network Toolbox of MATLAB 7 allows selecting the network type, number of hidden layers and hidden layer neurons, iterations during the model training and transfer functions. The non-linear function chosen was tan-sigmoid. The training algorithm used was Levenberg–Marquart and other parameters for network were chosen as the default values of the software. Weights were initialized with random values for training. Optimal network topology was determined by developing several networks that vary only with the size of hidden layer and simultaneously observing the change in the standard error.

3. Theoretical approach—electro-oxidation

The mechanism of electrochemical oxidation of wastewater is a complex phenomenon involving the coupling of electron transfer reaction with a dissociate chemisorption step. Basically two types of oxidative mechanism may occur at the anode; in the case of an anode with high electro-catalytic activity, oxidation occurs at the electrode surface, called direct electrolysis; in the other instances, for example metal oxide electrode, oxidation occurs via the surface mediator generated continuously on the anodic surface, called indirect electrolysis. In direct electrolysis, the rate of oxidation is depending on electrode activity, pollutants diffusion rate and current density. The electrochemical conversion/combustion of organics on noble oxide coated catalytic anode ($Ti/RuO_x–TiO_x$) can be explained as follows. In the first step, H_2O is discharged at the anode to produce adsorbed hydroxyl radicals according to the reaction,

$$(RuO_x–TiO_x) + H_2O \rightarrow (RuO_x–TiO_x)(^{\bullet}OH) + H^+ + e^- \quad (2)$$

In the second step, the adsorbed hydroxyl radicals may interact with the oxygen already present in the oxide anode with possible transition of oxygen from the adsorbed hydroxyl radical to the oxide to form the higher oxide ($RuO_x–TiO_{x+1}$).

$$(RuO_x–TiO_x)(^{\bullet}OH) \rightarrow (RuO_x–TiO_{x+1}) + H^+ + e^- \quad (3)$$

At the anode surface, active oxygen can be present in two states, either as physisorbed adsorbed hydroxyl radicals ($^{\bullet}OH$) or/and as chemisorbed (oxygen in the lattice ($RuO_x–TiO_{x+1}$)). In the absence of oxidizable organics, the active oxygen produces dioxygen according to the following reactions:

$$(RuO_x–TiO_x)(^{\bullet}OH) \rightarrow (RuO_x–TiO_x) + 1/2O_2 + H^+ + e^- \quad (4)$$

$$(RuO_x–TiO_{x+1}) \rightarrow (RuO_x–TiO_x) + 1/2O_2 \quad (5)$$

When NaCl is used as supporting electrolyte, chloride ion may anodically react with $(RuO_x–TiO_x)(^{\bullet}OH)$ to form adsorbed –OCl radicals according to the following reaction,

$$(RuO_x–TiO_x)(^{\bullet}OH) + Cl^- \rightarrow (RuO_x–TiO_x)(^{\bullet}OCl) + H^+ + 2e^- \quad (6)$$

Further, in presence of chloride ion, the adsorbed hypochorite radicals may interact with the oxygen already present in the oxide anode with the possible transition of oxygen from the adsorbed hypochlorite radical to the oxide, to form the higher oxide ($RuO_x–TiO_{x+1}$) according to the reaction given below. Simultaneously $(RuO_x–TiO_x)(^{\bullet}OCl)$ can react with the chloride ion to generate active oxygen (dioxygen) and chlorine according to the following reactions:

$$(RuO_x–TiO_x)(^{\bullet}OCl) + Cl^- \rightarrow (RuO_x–TiO_{x+1}) + Cl_2 + e^- \quad (7)$$

$$(RuO_x–TiO_x)(^{\bullet}OCl) + Cl^- \rightarrow (RuO_x–TiO_x) + 1/2O_2 + Cl_2 + e^- \quad (8)$$

In the presence of oxidizable organics, the physisorbed active oxygen ($^{\bullet}OH$) can cause predominantly the complete combustion of organics and chemisorbed will participate in the formation of selective oxidation [20,21] products according to the following reactions:

$$\tfrac{1}{2}R + (RuO_x - TiO_x)(^{\bullet}OH) \rightarrow \tfrac{1}{2}ROO + H^+ + e^- + (RuO_x - TiO_x) \quad (9)$$

$$R + (RuO_x–TiO_{x+1}) \rightarrow RO + (RuO_x–TiO_x) \quad (10)$$

The physisorbed route of oxidation is the preferable way for waste treatment. Since, the organic hydrogen peroxides formed are relatively unstable; decomposition of such intermediates will lead to molecular breakdown and the formation of subsequent intermediates with lower carbon numbers. These sequential reactions will continue until the formation of carbon dioxide and water [22,23]. In this case, the diffusion rate of organics on the anode area controls the combustion rate [24,25]. On the other hand, temperature, pH and diffusion rate of generated oxidants determine the rate of oxidation in indirect electrolysis. In the same way indirect electrochemical oxidation mechanism has been proposed for metal oxide with chloride as the supporting electrolyte for wastewater treatment [26–28]. The reactions of anodic oxidation of chloride ions to form chlorine in bulk solution as given by Eqs. (7) and (8) further proceeds as follows:

$$2Cl^- \xrightarrow{k_1} Cl_2 + 2e^- \quad (11)$$

$$Cl_2 + H_2O \xrightarrow{k_2} H^+ + Cl^- + HOCl \quad (12)$$

$$HOCl \underset{k_{3'}}{\overset{k_3}{\longleftrightarrow}} H^+ + OCl^- \quad (13)$$

$$\text{Organic} + OCl^- \xrightarrow{k_4} CO_2 + H_2O + Cl^- \quad (14)$$

Since organic compounds of the effluent are electrochemically inactive, the primary reaction occurs at the anodes is chloride ion oxidation [Eqs. (7) and (8)] with the liberation of Cl_2, which is a robust oxidizing agent. As regards the reactions in bulk, gaseous Cl_2 dissolves in the aqueous solutions due to ionization as indicated in equation (12). In cathode the following reactions takes place

$$2H_3O^+ + 2e^- \rightarrow H_2 + 2H_2O \quad \text{pH} > 7 \quad (15)$$

$$2H_2O + 2e^- \rightarrow H_2 + 2HO^- \quad \text{pH} < 7 \quad (16)$$

The rate of bulk reaction is less in acidic solution due to OH^- instability and considerably more in basic solution due to the ready formation of OCl^- (pK_a 7.44) ion in Eq. (13) implying that the basic or neutral pH conditions are more favorable for conducting reactions involving chlorine. The rate of direct electro-oxidation of organic pollutants depends on the catalytic activity of the anode, the diffusion rate of the organic compounds in the active points of anode and applied current density. The indirect electro-oxidation rate of organic pollutants depends on the diffusion rate of the oxidants into the solution, flow rate of the effluent, temperature and the pH. In moderate alkaline solutions, a cycle of chloride–chlorine–hypochlorite–chloride takes place, which produces OCl^-. The pseudo-steady state theory can be applied to each of the intermediate products (HOCl and OCl^-) in the bulk solution. The rate of reaction of the components can be written as

$$-r_{Cl_2} = k_2[Cl_2] \quad (17)$$

$$r_{HOCl} = k_2[Cl_2] - k_3[HOCl] + k_3'[H^+][OCl^-] = 0 \quad (18)$$

$$r_{OCl^-} = k_3[HOCl] - k_3'[H^+][OCl^-] - k_4[\text{organic}][OCl^-] = 0 \quad (19)$$

$$-r_{\text{organic}} = k_4[\text{organic}][OCl^-] \quad (20)$$

Then using the above equations we can easily deduce the following expression:

$$-r_{Cl_2} = -r_{\text{organic}} = k_4[\text{organic}][OCl^-] \quad (21)$$

Finally as regard to bulk solution it is also to be noted that $-r_{Cl_2} = r_{Cl}^-$ from Eq. (12), that is

$$-r_{Cl_2} = r_{Cl^-} = k_2[Cl_2] = -r_{\text{organic}} = k_4[\text{organic}][OCl^-] \quad (22)$$

where the rate of reaction r_i and the rate constants k_i (i = 2, 3 and 4) are defined with respect to the bulk. The rate expression for main electrode reaction as per Eq. (11) can be written as

$$-r'_{Cl^-} = r'_{Cl_2} = k_1[Cl^-] \quad (23)$$

where k_1 is the heterogeneous electrochemical rate constant.

In the following section an attempt is made to establish a relation between the reacting species in bulk and at the electrode surface. The basic relationship applicable to all electrochemical reactions is Faraday's law that relates to the amount of substance reacted on the surface to the charge ($I_A t$) passed, $M_A I_A t/nF$ (assuming 100% current efficiency) and the characteristic measurable parameter, current density, i_A (defined as I_A/A_e). Thus, the electrochemical reaction rate (for the disappearance of reactant A) can be expressed as

$$-\left(\frac{V_R}{A_e}\right)\frac{d[A]}{dt} = \frac{i_A}{nF} \quad (24)$$

where I_A is the current passed in time t, M_A is the molecular weight, n is the number of electrons transferred per mole of reaction, A_e electrode area, V_R reactor volume and F is the Faraday constant (96,485.3 C/mol). It has to be noted that $-r_A = -d[A]/dt = i_A a/nF$ where a is specific electrode area (A_e/V_R). Assuming the main electrode reaction, governed by a simple Tafel type expression,

$$-\left(\frac{V_R}{A_e}\right)\frac{d[A]}{dt} = \frac{i_A}{nF} = k'[A]\exp(bE) \quad (25)$$

or

$$-r'_{Cl^-} = r'_{Cl_2} = k_1[Cl^-] = k_1' a[Cl^-]\exp(bE) \quad (26)$$

The reaction may be assumed to be under diffusion control as the reacting species, Cl^- in the electrolyte is dilute. The reactant Cl^- is transported from the bulk to electrode surface where it undergoes electrochemical oxidation to Cl_2 and it may be transported back to the bulk by diffusion reaction in the bulk. Then,

$$\frac{i_A}{zF} = k_L([Cl^-] - [Cl^-]_s) \quad (27)$$

Elimination of $[Cl^-]_s$ using Eqs. (17) and (18),

$$\frac{i_A}{zF} = k_1[Cl^-] \quad (28)$$

where

$$\frac{1}{k_1} = \frac{1}{k_L} + \frac{1}{k' a \exp(bE)} \quad (29)$$

From a material balance of species Cl^- by taking note of Eqs. (13) and (14) we can write

$$\frac{i_A}{zF} = k'[Cl_2] \quad (30)$$

$$\frac{i_A}{zF} = k''[\text{organic}][OCl^-] \quad (31)$$

During electrolysis, if constant current is applied, the rate of generation of $[OCl^-]$ will remain constant under a given set of experimental condition, but will vary if the applied current is altered. Then,

$$\frac{i_A}{zF} = k_{obs}[\text{organic}] = k[\text{COD}] = kC \quad (32)$$

3.1. Batch reactor

Adopting the same classification for the reactors as for conventional reactors, the electrochemical reaction rate (for removal of COD) in batch reactor can be expressed as

$$-\left(\frac{V_R}{A_e}\right)\frac{dC}{dt} = \frac{i_A}{zF} = k_L C \quad (33)$$

$$C = C_o\exp(-k_L a t) \quad (34)$$

or integrated form $-\ln\left[\frac{C}{C_o}\right] = k_L a t$

In electrochemical conversion, the high molecular weight aromatic compounds and aliphatic chains are broken to intermediate products for further processing. In electrochemical combustion, the organics are completely oxidized to CO_2 and H_2O. The progress of the destruction of the organic pollutant was monitored by COD estimation. The potentials required for oxidation of organic pollutants are generally high and the production of oxygen from the electrolysis of water molecules may determine the reaction yield. The current efficiency of the electrolysis can be calculated using the following expression.

$$\text{current efficiency (CE)} = \frac{V_R \Delta C \times 10^{-3}}{(16It/2F)} \times 100 \quad (35)$$

where ΔC is the difference in COD in mg L^{-1}, due to the treatment by passing I current for t seconds. V_R is volume of the reactor (liters).

Q represents the volumetric flow rate in L s^{-1} and F, Faraday's constant. Current efficiency can be defined as the ratio of milligrams of oxygen demand removed by the passage of a given charge of electrical energy to the equivalent milligrams of oxygen predicted by Faraday's law. During electrochemical degradation of organic matter COD removal is not due to oxidation by molecular oxygen alone. A number of other strong oxidizing agents (as explained before) are generated in situ which play major role in the destruction of the organic matter. So it is not possible to expect the current efficiency figures in the range of 0–100%.

While current efficiency indicates the fraction of the total current passed for the targeted reaction, the term, specific energy consumption (SEC) is the quantity of energy consumed in the process for a kg of COD to get digested. The term (in kW h kg^{-1}) for batch reactor can be obtained using the equation,

$$\text{specific energy consumption (SEC)} = \frac{VIt}{3600 \times 10^3} \times \frac{1}{\Delta C \times V_R \times 10^{-6}} \tag{36}$$

where V represents the applied cell voltage in volts and the remaining terms are as defined above.

3.2. Batch reactor with recirculation mode

As the flow through the reactor only in axial direction and the dispersion number is very low, plug flow exists in the present in case of flow reactor. It was arrived based on residence time distribution (RTD) tracer experiment. An approximate model may be described by a plug flow reactor (PFR) in which the reactions take place. A dynamic material balances to each of component or species can be written as

[rate of change mass of species in the reactor]

= [rate of mass input] − [rate of mass output]

$\mp \sum$ [rate of mass of species disappeared or generated physicochemical phenomena]

The concentration variation of organic in the differential volume of reactor (see Fig. 2) can be written as

$$-A\ \Delta x \left(\frac{\partial C'}{\partial t}\right) = Q\left(\frac{\partial C'}{\partial x}\right)\Delta x + A\,\Delta x\, k_L a\, C' \tag{37}$$

LHS represents the rate of change of COD in the differential volume of reactor, $A\,\Delta x$ where A is the cross-section area of the reactor. The first term of the RHS is the net rate of change of COD due to the bulk flow in the differential volume and Q is the volumetric flow rate through the reactor. The last term in the right-hand side represents the rate of degradation of organic contaminants the solution due to reaction.

Considering the reservoir to be a perfectly back-mix system, the mass balance of the species across the reservoir can be written as:

$$V\left(\frac{dC}{dt}\right) = QC' - QC \tag{38}$$

Further it can also be assumed that the reactor is under steady state condition as $dC'/dt = 0$, and rewrite Eq. (33) as

$$C' = C\exp(-k_L a\tau_R) = C\exp\left(-\frac{k_L A_e}{Q}\right) \tag{39}$$

where a is specific electrode area (A_e/V_R) and τ_R is the residence time (V_R/Q) in the reactor. The mass balance equation can be solved after substitution of the expression for C', knowing the initial COD, the resultant equation can be written as

$$\frac{C}{C_o} = \exp\left[-\frac{t}{\tau}(1-\exp(-k_L a\tau_R))\right] = \exp\left[-\frac{t}{\tau}\left\{1-\exp\left(\frac{-k_L A_e}{Q}\right)\right\}\right] \tag{40}$$

where C_o is the initial value of COD of waste water and τ is the residence time (V/Q) in the reservoir.

It should be noted that the extent of degradation is defined as $X = (C_o - C)/C_o$. The unconverted species $(1 - X)$, (or C/C_o), decreases exponentially with time. According to Eq. (40), the slope of the plot of $-\ln(1-X)$ versus t, gives the value $\left\{1-\exp(-k_L A_e/Q)\right\}/\tau$ from which the value of k_L, the rate transfer coefficient, may be computed.

The current efficiency (CE) and specific energy consumption (SEC) figures for flow reactors are obtained using the following expressions.

$$\text{current efficiency (CE)} = \frac{Q\,\Delta C \times 10^{-3}}{(16I/2F)} \times 100 \tag{41}$$

$$\text{specific energy consumption (SEC)} = \frac{VI}{3600 \times 10^3} \times \frac{1}{\Delta C \times Q \times 10^{-6}} \tag{42}$$

3.3. Recycle reactor

For the recycle reactor system, streams 10 and 12 will be present and the material balance around the reservoir will give concentration of the reactant entering the reactor as,

$$C = \frac{qC_0 + QC'}{q+Q} = \frac{RC_0 + C'}{R+1} \tag{43}$$

where q is the volumetric inlet/discharge flow rate, and R is the ratio, defined as $R = q/Q$ and Q, the bulk flow rate of the effluent circulating and entering the reservoir all the time. The material balance around the reactor,

$$C' = C\ \exp(-k_L a\tau_R) = C\exp\left(-\frac{k_L A_e}{Q+q}\right) \tag{44}$$

where $Q + q$ is the total flow of effluent passing through the reactor. In Eq. (40) substituting for C' from the above expression, we get

$$C = \frac{RC_0 + C\ \exp(-(k_L A_e)/(Q(1+R)))}{R+1} \tag{45}$$

The above equation can be rearranged in the following form.

$$\left(\frac{k_L A_e}{Q(1+R)}\right) = \ln\left(\frac{1-X}{(R+1)(1-X)-R}\right) \tag{46}$$

According to Eq. (46), the slope of the plot $\ln((1-X)/((R+1)(1-X)-R))$ versus $1/(1+R)Q$, gives the value $k_L A_e$ from which the value of k_L, the rate transfer coefficient, may be computed for the given conversion in the recycle reactor.

4. Results and discussion

The results of the experiments carried out are presented in Figs. 3–6. Preliminary batch experiments show that the electrolysis time, supporting electrolyte concentration and current density considerably influence the performance of the process. Process performance is defined in two ways, one with respect to the extent of reaction completion (X or % COD removal) of the process and the other with respect to the specific energy consumption, SCE (kW h kg^{-1}) in the process. Rate of the process, determined by the current density (Eq. (32)), is evaluated in terms of the heterogeneous rate constant k_L (cm s^{-1}) by monitoring the extent of COD

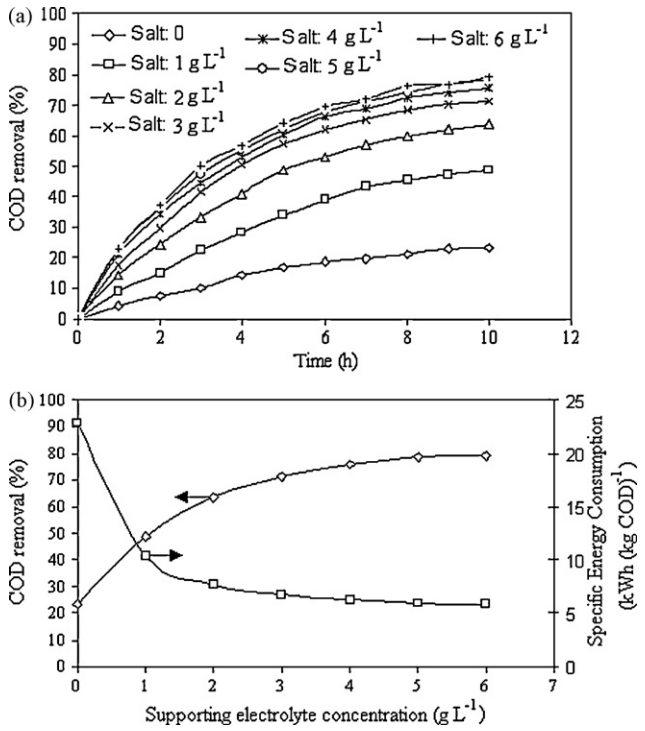

Fig. 3. The effect of supporting electrolyte concentration on performance of the process in batch reactor. *Conditions*: current density of 4 A dm^{-2}, initial COD: 17,750 mg L^{-1}, pH 7, specific electrode surface: 0.128 cm^{-1}, duration: 10 h, volume of effluent treated: 200 mL. (a) Variation of COD removal (%) and (b) variation of COD removal (%) and specific energy consumption.

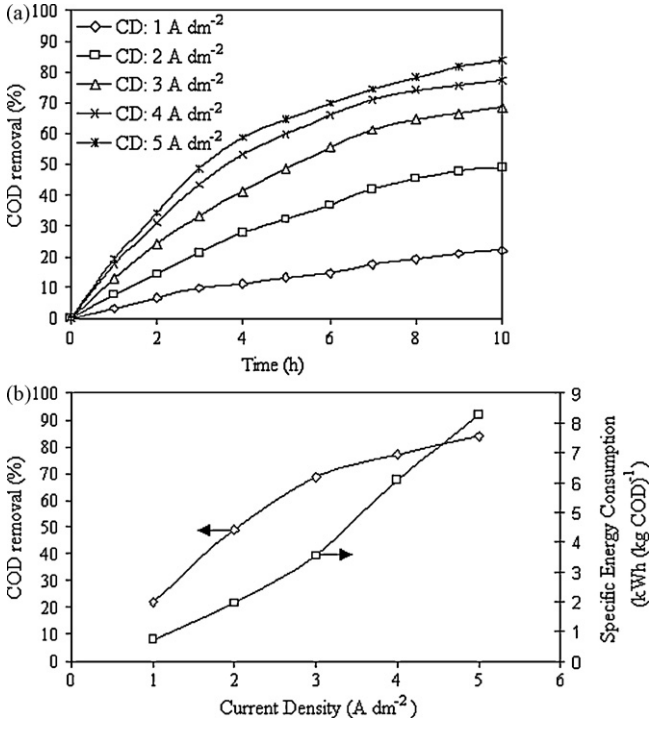

Fig. 4. The effect of current density on performance of the process in batch reactor. (a) Variation of COD removal (%) and (b) variation of COD removal (%) and specific energy consumption. (All conditions are same as Fig. 3 except supporting electrolyte concentration 5 g L^{-1}.)

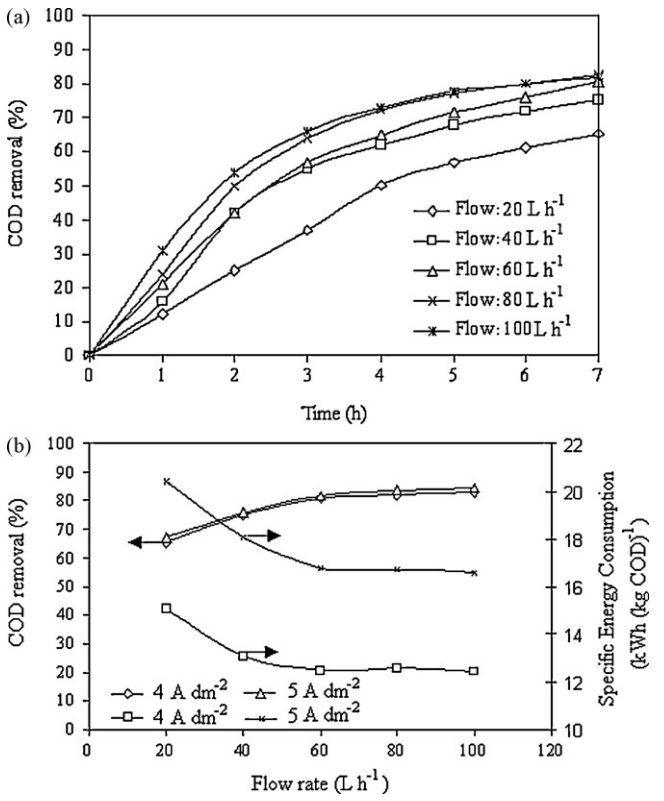

Fig. 5. Effect of current density and flow rate on the performance of the process in batch recirculation reactor. (a) Variation of COD removal (%) and (b) variation of COD removal (%) and specific energy consumption. *Conditions*: supporting electrolyte concentration: 5 g L^{-1}, initial COD: 17,750 mg L^{-1}, pH 7, volume of effluent treated: 2000 mL, and specific electrode surface: 0.145 cm^{-1}.

removal. The energy consumption is also defined in two ways. The current efficiency computation indicates the path and course of the targeted reaction by monitoring the extent of COD removal (Eq. (35)). The actual utilization of energy in fulfilling unit quantity of the targeted reaction (specific energy consumption, SCE, kW h (kg COD)$^{-1}$), is found by monitoring the cell voltage and extent of COD removal (Eq. (36)). The results of detailed batch experiments are reported in Figs. 3 and 4. Batch studies were useful in determining the operating parameters such as electrolysis duration, supporting electrolyte concentration and current density giving better rector performance.

Fig. 3a indicates the variation of the extent of the removal of organic contaminants (in terms of COD) with electrolysis duration for various supporting electrolyte concentrations at a current den-

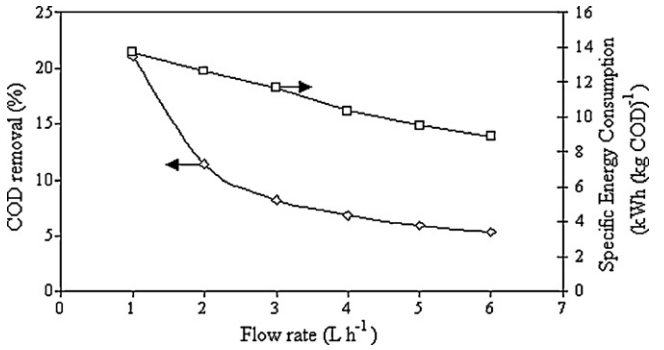

Fig. 6. Effect of withdrawal flow rate on the performance of recycle reactor. *Conditions*: current density: 4 A dm^{-2}, recycle flow rate: 20 L h^{-1} and other relevant conditions as in Fig. 5.

sity of 4.0 A dm^{-2}. It can be seen from the figures that the rate of change of completion of the process decreases exponentially as the process progresses especially at situations of higher salt levels. The expected increase in pollutant removal performance beyond 8 h of treatment is marginal. It can also be observed from the figures that the supporting electrolyte plays a major role in the degradation of the organic matter present in the wastewater. Even though the pollutant removal performance of the system increases an increase in salt levels, the change in the performance decreases as the salt concentration increases. As can be read from Fig. 3b, increase in supporting electrolyte concentration from 1 to 2 g L^{-1} resulted in an improvement from 48.6% to 63.7% in COD removal after 10 h of treatment. But the same improvement was very less (from 78.6% to 79.1%) due to an increase in the supporting electrolyte concentrations at higher levels, i.e., from to 5 to 6 g L^{-1}. The performance of the process due to salt concentration was found to improve only marginally beyond 5 g L^{-1}. Since the post-treatment for removal of the dissolved inorganic substances is cumbersome, the salt level in the wastewater has to be limited. Moreover, current density is a direct measure of the energy consumption of the process and thus, has to be limited for better overall economics of the process.

The trend of heterogeneous rate constant k_L (cm s^{-1}) with respect to the variation of current density and supporting electrolyte concentration was also studied in batch mode of operation. There is a marked improvement in the value of k_L with an increase in salt concentration, especially at lower salt levels (1.45×10^{-4} cm s^{-1} at 1 g L^{-1} to 2.21×10^{-4} cm s^{-1} at 2 g L^{-1}), probably due to the generation of more oxidizing agents from the additional amount of salt added in the effluent. With the addition of extra salt, the controlling step of the process might have changed over from a condition of limiting oxidizing agents to any other limiting condition, such as limiting organic species. As can be seen in Fig. 3b, an increase in salt concentration improves the specific energy consumption of the process, especially at lower salt concentrations. This may be due to the improved ionic conductance of wastewater.

The effect of current density on the performance of the process is also studied; the results are presented in Fig. 4a and b. Both the figures shows that the improvement in process performance is marginal for current density more than 4 A dm^{-2}. It was also noticed that an increase in current density increases the specific energy consumption. The possibility of loss of electrical energy in the form of heat and for unwanted reactions is more at high levels of current density. Thus, in general, a higher current density operation will give high capacity utilization, at the expense of more energy loss.

In this investigation, for indirect electrochemical degradation of organic contaminants, the current efficiencies increased above 100%. In the electrochemical degradation of pulp and paper mill wastewater, Mishra and co-workers [29] had reported current efficiencies ranging from 400% to 500% and others [30] reported current efficiency increases above 100%. Again it should be noted that COD is not a chemical compound to follow Faraday's law in a thermodynamic sense. These higher value efficiencies may only indicate that there exists a large chemical reaction and physical processes such as adsorption to contribute to COD reduction. Here formation of strong oxidising agents such as chlorine (Cl_2), hypochlorite (OCl^-), and chlorate (ClO_3^-) may occur and these intermediate products may chemically oxidize organic contaminants of effluent in a long period of electrolysis.

4.1. Batch reactor with recirculation mode

Dynamic response of the COD removal performance of the system was studied at various flow rates, Q at constant conditions of current density (4 A dm^{-2}), supporting electrolyte concentration (5 g L^{-1}) and initial COD (17,750 mg L^{-1}); the result is presented in Fig. 5a and b. There is an increase in percentage of COD removal of the process with respect to time as shown in Fig. 5a. The improvement in process performance after 7 h of operation is marginal. It can also be seen in the figure that the pollutant removal performance of the system improves considerably with an increase in the flow rate. As can be seen in Fig. 5b, the COD removal of the system after 7 h of operation was found to be 65.3% and 82.7% at circulation flow rates of 20 and 100 L h^{-1} respectively at a current density of 4 A dm^{-2}. This may because of the enhancement of the transfer coefficient at higher flow rates. Pollutant removal performance and energy consumption performance of the system were studied with respect to the variation of flow rates for treatment duration of 7 h at constant conditions as explained above; the results are presented in Fig. 5b.

The improvement in COD removal (65.3–82.7%) resulted in considerable improvement in current efficiency, CE (95.6–121.1%) and specific energy consumption, SCE (15.06–12.45 kW h kg^{-1}) figures of the system when the flow rate (Q, L h^{-1}) increased from 20 to 100 L h^{-1} at a current density of 4 A dm^{-2}. This may because of the improved ionic conductivity by bulk movement and with the reduction of resistance on the electrode surface. The quantity of pollutant removed as been improved by 3.8 times; by this change in flow rate. It has been tried to correlate the mass transfer coefficient with the velocity of effluent flowing through the reactor, in the form,

$$k_L = m\,u^n \tag{47}$$

By graphical solution of the above equation the values of m and n are obtained as 4.44 and 0.362 respectively for operation at a current density of 4 A dm^{-2}. This observation indicates that the k_L for the flow channel may be expressed theoretically using a Leveque-type Eq. [31] in which k_L is dependent on $u^{0.33}$.

4.2. Recycle reactor

The pollutant removal and energy consumption performance of the recycle reactor was studied for various influent/withdrawal flow rates (q, L h^{-1}) at a recycle flow rates (Q, L h^{-1}) of 20; the results are presented in Fig. 6. An increase in withdrawal flow rate decreases the COD removal. The percentage of COD removals reported at 1 and 6 L h^{-1} are reported as 21% and 5.3% respectively. This may be due to the shorter residence time at higher withdrawal flow rates. The improvement in the power consumption at higher withdrawal flow rates can be seen in Fig. 6. There is considerable increase in the value of k_L as the withdrawal flow rate increases (0.009 cm s^{-1} at 1 L h^{-1} to 0.056 cm s^{-1} at 6 L h^{-1}). In general, the operation of the reactor at higher withdrawal flow rates provides better capacity utilization with better energy figures, but at the expense of poor completion of the process. When compared with batch recirculation reactor, recycle reactor performance is found to be attractive on power consumption figures and heterogeneous rate constant. Recycle reactor is found to be better configuration, because of its flexibility of operation. Circulation flow rate and withdrawal flow rate enable control on transfer coefficients and treatment duration respectively. Thus the recycle reactor is more apt for process integration.

4.3. Artificial neural network

In order to demonstrate use of ANN in predicting the performance of batch electrochemical reactor, six numbers of back-propagation neural networks, BPNN (see Table 1) have been tested and the results are presented in Tables 2 and 3 and Figs. 7 and 8. Various neural networks were selected based on the number of weights to be determined and the available number of data for training [32]. Table 1 shows the configurations of the networks studied-three

Table 1
Configurations of the neural networks studied.

BPNN abbreviation	Configuration
N1	3-5-1
N2	3-7-1
N3	3-9-1
N4	3-3-3-1
N5	3-3-5-1
N6	3-3-7-1

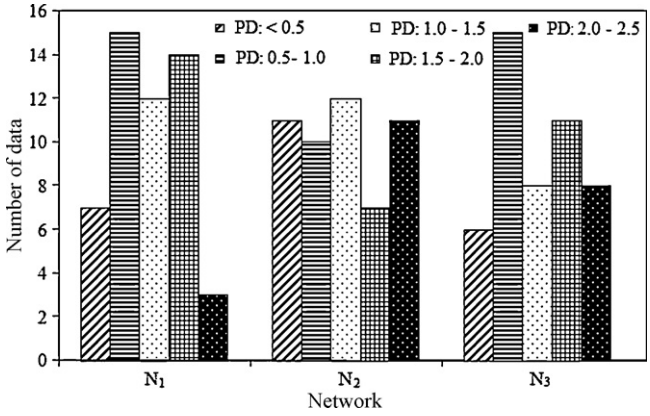

Fig. 7. Number of data points in five percentage deviation ranges for the case of three layered networks in predicting the COD removal (%) in batch reactor.

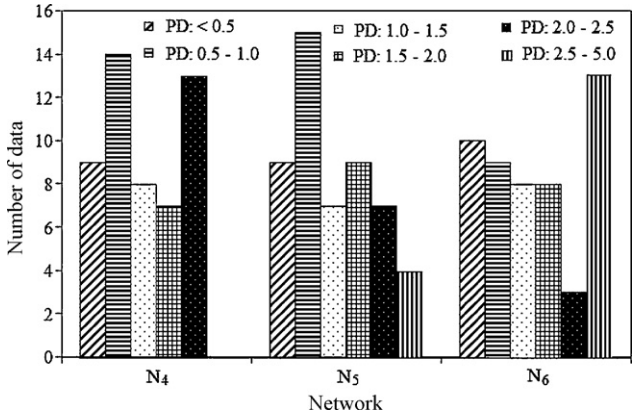

Fig. 8. Number of data points in six percentage deviation ranges for the case of four layered networks in predicting the COD removal (%) in batch reactor.

Table 3
Standard statistical evaluation during validation of the model performance.

	N1	N2	N3	N4	N5	N6
R	0.9982	0.9977	0.9979	0.9982	0.9982	0.9960
AARE (%)	1.1934	1.2313	1.2695	1.2575	1.2621	1.6128
RMSE	0.7624	0.8378	0.8322	0.8629	0.8641	1.1703
NMBE (%)	−0.1694	0.0105	−0.2732	−0.5857	−0.5450	0.4632
SI	0.0129	0.0142	0.0141	−0.5857	−0.5450	0.4632

numbers of single hidden layer cases and three numbers of double hidden layers cases were considered for the investigation. Totally, 125 data were collected in random combination of factors in the experimental domain for the development of ANN model. The one combination of variables, given complete COD removal, was not considered for the ANN analysis. The remaining 124 experimental data were randomly divided into two sets. One set, 100 nos., was used for training and the other, 24 data, was used for testing the model.

Several iterations were conducted with different numbers of neurons of hidden layer in order to determine the best ANN structure. The trial started with the case of single hidden layer. The number of neurons in the hidden layer is varied for 3, 7 and 9; the corresponding networks are notated N1, N2 and N3 respectively. The least standard error value and a good prediction of the outputs of both training and validation sets were obtained with 7 neurons in the hidden layer (N2). The cases of 10 and more neurons in the hidden layer were not giving consistent results.

Table 2
Test of the ANN models.

CD	Time	Salt	Expt.	N1	N2	N3	N4	N5	N6
4.5	4.5	4.5	66.74	67.24	66.87	66.65	67.70	67.58	67.23
4.5	7	5.75	82.57	82.75	82.79	82.27	82.77	81.93	81.66
2	3.25	2	12.37	13.65	13.37	13.36	14.14	12.85	15.72
3.25	2	5.75	32.48	32.68	32.54	32.77	32.98	32.51	32.52
2	3.25	5.75	32.52	32.20	32.65	32.55	32.47	32.34	32.98
2	4.5	2	25.19	26.19	25.13	25.77	26.41	25.22	27.66
5.75	2	3.25	40.96	40.18	40.11	40.50	39.93	40.57	39.14
4.5	2	7	44.14	44.59	45.00	44.63	44.67	45.00	46.79
4.5	4.5	5.75	70.14	70.09	69.85	70.29	70.21	70.07	69.64
5.75	5.75	3.25	76.03	76.16	76.62	75.56	76.21	75.69	74.95
3.25	7	7	70.41	71.28	71.06	71.36	70.68	71.25	71.14
3.25	4.5	2	40.89	40.84	40.05	41.06	40.75	41.02	40.95
5.75	3.25	5.75	65.18	65.98	66.31	65.91	65.59	65.65	66.51
4.5	2	5.75	43.94	44.36	44.24	44.34	44.48	44.36	44.74
3.25	4.5	7	58.73	58.98	58.84	58.19	58.81	59.04	58.29
7	5.75	7	85.41	84.27	83.98	84.44	84.77	84.35	84.73
4.5	2	2	22.88	22.96	22.57	23.64	22.35	22.11	21.29
3.25	3.25	4.5	44.50	44.30	44.20	43.55	44.52	44.59	42.40
7	5.75	2	70.38	70.34	70.31	70.77	70.41	70.25	70.32
3.25	4.5	3.25	49.58	50.19	49.62	50.22	49.98	50.31	49.88
7	4.5	3.25	70.12	70.13	69.61	69.93	70.20	69.98	68.85
2	5.75	5.75	53.11	52.28	52.55	51.91	52.14	51.66	53.03
5.75	4.5	5.75	76.75	76.58	76.77	76.52	76.35	76.73	76.74
5.75	2	7	51.34	51.53	51.58	51.46	51.46	51.53	51.52
Slope				1.009	1.005	1.013	1.011	1.005	1.024
Intercept				−0.87	−0.47	−0.98	−0.93	−0.49	−1.57
R^2				0.997	0.998	0.998	0.998	0.998	0.995
Standard error				0.93	0.86	0.89	0.95	0.90	1.41

Standard error is defined by

$$\sqrt{\frac{1}{(n-2)}\left[\sum(y-\bar{y})^2-\frac{\left[\sum(x-\bar{x})(y-\bar{y})\right]^2}{\sum(x-\bar{x})^2}\right]} \quad (48)$$

The performance of ANN models of two hidden layer cases, 3-3-3-1, 3-3-5-1 and 3-3-7-1 (notated N4, N5 and N6 respectively) were also studied. The test results along with their performance terms such as slope, intercept, R^2 and standard error are presented in Table 2. Each network is tested for its ability in predicting the performance of the process by comparing prediction with 51 numbers of experimental observations. The results for three and four layered networks are presented in Figs. 7 and 8 respectively. The predictability of the network is again quantified in terms of standard statistical performance evaluation measures such as correlation coefficient (R), average absolute relative error (AARE), average root mean square error (RMSE), normalized mean bias error (NMBE) and scatter index (SI), expressed as:

$$R=\frac{\sum_{i=1}^{N}(E_i-\bar{E})(P_i-\bar{P})}{\sqrt{\sum_{i=1}^{N}(E_i-\bar{E})^2\sum_{i=1}^{N}(P_i-\bar{P})^2}} \quad (49)$$

$$\text{AARE}\ (\%)=\frac{1}{N}\sum_{i=1}^{N}\left|\frac{(E_i-P_i)}{E_i}\right|\times 100 \quad (50)$$

$$\text{RMSE}=\left[\frac{1}{N}\sum_{i=1}^{N}(P_{ij}-E_{ij})^2\right]^{1/2} \quad (51)$$

$$\text{NMBE}\,(\%)=\frac{(1/N)\sum_{i=1}^{N}(E_i-P_i)}{(1/N)\sum_{i=1}^{N}E_i}\times 100 \quad (52)$$

$$\text{SI}=\frac{\text{RMSE}}{\bar{E}} \quad (53)$$

where E is the experimental finding and P is the predicted value obtained from the neural network model. $\bar{E}$ and $\bar{P}$ are the mean values of E and P respectively. N is the total number of data employed in the investigation. The statistical terms of the networks are presented in Table 3. It can be read from Figs. 7 and 8 and their performance terms, given in Table 3, that N2, N3 and N5 are comparably better in predicting the COD removal of the process. The correlation coefficient is a commonly used statistic and provides information on the strength of linear relationship between observed and the computed values. Sometimes higher value of R may not necessarily indicate better performance of ANN model [33] because of the tendency of the model to be biased towards higher or lower values. The AARE and RMSE are computed through a term-by-term comparison of the relative error and therefore are unbiased statistics for measuring the predictability of a model [34]. The NMBE gives information on the mean bias in prediction from a model. Positive NMBE indicates over prediction whereas negative indicates under prediction from a model. In the case of three layered networks, increase in number of neurons in the hidden layer enhanced the performance of the network. But in the case of four layered networks the trend is found reverse.

It can be concluded that single hidden layer network is adequate enough to predict the performance of the process. This observation reaffirms the universal approximation theorem that a single layer of non-linear hidden units is sufficient to approximate any continuous function. Hornik et al. [35] have also shown that a three layer ANN with sigmoid transfer function can map any function of practical interest.

This work addresses an important problem of electrochemical wastewater treatment. The process is a reasonably well behaved electrochemical system, and we have calculated reaction rate constants as a function of current (so it is electrochemical reaction rate constant) and as a function of flow rate (mass transfer limited rate constant). With this information, the model will be able to predict the effect of flow rate, current, concentration etc. on the current and energy efficiencies. Therefore, one may think the need for ANN is not justified. The intention of the ANN section in the paper is just to indicate that as and when the real effluent was collected from industry, experiments were carried out and concept of ANN was applied and updated independently well before the process mathematical description of the phenomena of started. Therefore this methodology might prove useful in simulating and up-scaling still more complex electrochemical systems.

5. Conclusions

Electrochemical degradation of wastewater from a medium-scale, specialty chemical industry was investigated using $Ti/RuO_x–TiO_x$ anode in various types of reactor configurations such as batch, batch recirculation and continuous recycle systems. The effect of important operating parameters such as current density, electrolysis time and supporting electrolyte concentration on the pollutant removal and energy consumption performance of these systems are critically examined.

Batch studies show the operating parameters as current density: $4\,A\,dm^{-2}$, electrolysis duration: 6 h, supporting electrolyte concentration: $5\,gm\,L^{-1}$, as optimal for better overall performance of the system. The pollutant removal performance of the batch recirculation system was to improve considerably with an increase in the circulation flow rate. The improvement in COD removal (65.3–82.7%) resulted in considerable improvement in current efficiency, CE and specific energy consumption, SCE ($15.06–12.45\,kW\,h\,kg^{-1}$) figures of the system when the flow rate (Q, $L\,h^{-1}$) increased from 20 to $100\,L\,h^{-1}$ at a current density of $4\,A\,dm^{-2}$. When compared with batch recirculation reactor, recycle reactor performance is found to be attractive on power consumption figures and rate constant. Recycle reactor is found to be better configuration, because of its flexibility of operation. Circulation flow rate and withdrawal flow rate enable control on transfer coefficients and treatment duration respectively. Thus the recycle reactor is more apt for commercial applications. The performance of COD removal in the batch reactor is predicted using ANN. Single hidden layer feed forward back-propagation neural network is found adequate enough to predict the performance of the process. Complete mineralization such a heavily loaded organic effluent cannot anyway, be economically viable. The present investigation is helpful in estimating and comparing the energy demanded by the conventional reactor configurations in destructing the organic part of a typical high strength organic waste. The integration of this environment friendly treatment technique with other similar treatments such as biological treatment, connected multiple units alternatively in series, for improvement of biodegradability, with a fraction of the energy demanded by the electrochemical treatment will a viable technique.

References

[1] N.C. Shang, Y.H. Yu, Toxicity and color formation during ozonation of mono substituted aromatic compounds, Environ. Technol. 23 (2002) 43–52.
[2] S. Ledakowicz, M. Solecka, R. Zylla, Biodegradation, decolourisation and detoxification of textile wastewater enhanced by advanced oxidation processes, J. Biotechnol. 89 (2001) 175–184.
[3] E. Chamarro, A. Marco, S. Esplugas, Use of Fenton reagent to improve organic chemical biodegradability, Water Res. 35 (2001) 1047–1051.
[4] S. Parra, S. Malato, C. Pulgarin, New integrated photocatalytic–biological flow system using supported TiO_2 and fixed bacteria for the mineralization of isoproturon, Appl. Catal. B: Environ. 36 (2002) 131–144.

[5] M.H. Entezari, C. Pétrier, A combination of ultrasound and oxidative enzyme: sono-biodegradation of substituted phenols, Ultrason. Sonochem. 10 (2003) 241–246.
[6] J.B. Rodr'ıguez, A. Mutis, M.C. Yeber, J. Freer, J. Baeza, H.D. Mansilla, Chemical degradation of EDTA and DTPA in a totally chlorine free (TCF) effluent, Water Sci. Technol. 40 (1999) 267–272.
[7] J. Bandara, C. Pulgarin, P. Périgner, J. Kiwi, Chemical (photo-activated) coupled biological homogeneous degradation of *p*-nitro-*o*-toluene-sulfonic acid in a flow reactor, J. Photochem. Photobiol. A: Chem. 111 (1997) 253–263.
[8] P. Hörsch, A. Speck, F.H. Frimmel, Combined advanced oxidation and biodegradation of industrial effluents from the production of stilbene-based fluorescent whitening agents, Water Res. 37 (2003) 2748–2756.
[9] C.A. Basha, E. Chithra, N.K. Sripriyalakshmi, Electro-degradation and biological oxidation of non-biodegradable organic contaminants, Chem. Eng. J. 149 (2009) 25–34.
[10] P. Cañizares, C. Sáez, J. Lobato, M.A. Rodrigo, Electrochemical treatment of 2,4-dinitrophenol aqueous wastes using boron-doped diamond anodes, Electrochim. Acta 26 (2004) 4641–4650.
[11] P. Cañizares, R. Paz, C. Sáez, M.A. Rodrigo, Electrochemical oxidation of alcohols and carboxylic acids with diamond anodes: a comparison with other advanced oxidation processes, Electrochim. Acta 5 (2008) 2144–2153.
[12] M. Zhou, J. He, Degradation of azo dye by three clean advanced oxidation processes: wet oxidation, electrochemical oxidation and wet electrochemical oxidation—a comparative study, Electrochim. Acta 4 (2007) 1902–1910.
[13] M Faouzi, P. Cañizares, A. Gadri, J. Lobato, B. Nasr, R. Paz, M.A. Rodrigo, C. Saez, Advanced oxidation processes for the treatment of wastes polluted with azoic dyes, Electrochim. Acta 1 (5) (2006) 325–331.
[14] K. Rajeshwar, J.G. Ibanez, Environmental Electrochemistry Fundamentals and Applications in Pollution Abatement, Academic Press, San Diego, CA, 1997, pp. 362–363.
[15] S. Rao, S. Mandal, Hind casting of storm waves using neural networks, Ocean Eng. 32 (2005) 667–684.
[16] L.S. Clesceri, A.E. Greenberg, A.D. Eaton, Standard Methods for the Examination of Water and Wastewater, 20th ed., APHA, Washington, DC, 1998.
[17] P. Subbiah, S. Krishnamurthy, K. Asokan, K. Subramanian, V. Arumugam. An improved process for the preparation of insoluble non-precious metal oxide anode doped with platinum group metal oxide to be used in electrochemical processes, Indian Patent 178184, 1990.
[18] M.A. Hussain, M. Shafiur Rahman, C.W. Ng, Prediction of pores formation (porosity) in foods during drying: generic models by the use of hybrid neural network, J. Food Eng. 51 (2002) 239–248.
[19] S. Aber, N. Daneshvar, S.M. Soroureddin, A. Chabok, K. Asadpour-Zeynali, Study of acid orange 7 removal from aqueous solutions by powdered activated carbon and modeling of experimental results by artificial neural network, Desalination 211 (2007) 87–95.
[20] M. Panizza, A.P. Michaud, G. Cerisola, C. Comninellis, Electrochemical treatment of wastewater containing organic pollutants on boron doped diamond electrode: prediction of specific energy consumption and required electrode area, Electrochem. Commun. 3 (7) (2001) 336–339.
[21] O. Simond, V. Schaller, C. Comninellis, Theoretical model for the anodic oxidation of organics on metal oxide electrodes, Electrochim. Acta 42 (1997) 2009–2012.
[22] G.R.P. Malpass, A.J. Motheo, Electro-oxidation of formaldehyde methanol solutions on $Ti/Ru_{0.3}Ti_{0.7}O_2$ electrodes using a filter-press cell, J. Appl. Electrochem. 31 (2001) 1351–1357.
[23] K. Bindu, S. Velusamy, C.A. Basha, R. Vijayavalli, Mediated electrochemical oxidation of organic pollutants in wastewater treatment, Indian J. Environ. Health 4 (2000) 185–191.
[24] S. Raghu, C.A. Basha, Electrochemical treatment of procion block 5B using cylindrical flow reactor—a pilot plant study, J. Hazard. Mater. 139 (2) (2007) 381–390.
[25] A. Buso, L. Balbo, M. Giomo, G. Farnia, G. Sandona, Electrochemical removal of tannins from aqueous solutions, Ind. Eng. Chem. Res. 39 (2000) 494–499.
[26] C. Comninellis, C. Pulgarin, Electrochemical oxidation of phenol for wastewater treatment using SnO_2 anodes, J. Appl. Electrochem. 23 (1993) 108–112.
[27] D.W. Miwa, G.R.P. Malpass, S.A.S. Machado, A.J. Motheo, Electrochemical degradation of carbaryl on oxide electrodes, Water Res. 40 (2006) 3281–3289.
[28] G.R.P. Malpass, D.W. Miwa, D.A. Mortari, S.A.S. Machado, A.J. Motheo, Decolorisation of real textile waste using electrochemical techniques: effect of the chloride concentration, Water Res. 41 (2007) 2969–2977.
[29] S. Mahesh, B. Prasad, I.D. Mall, I.M. Mishra, Ind. Eng. Chem. Res. 45 (2006) 2830.
[30] G. Chen, Sep. Purif. Technol. 38 (2004) 11.
[31] P. Robertson, P. Cettou, D. Matic, F. Schwager, A. Strorck, N. Ibl, in: M. Krumpelt, E.V. Weissman, R.C. Alkire (Eds.), Electro Organic Synthesis Technology: AIChE Symposium Series No. 185, 1979, p. 115, New York.
[32] W. Sha, Comments on the issues of statistical modeling with particular reference to the use of artificial neural networks, Appl. Catal. A: Gen. 324 (2007) 87–89.
[33] P. Phaniraj, A.K. Lahiri, The applicability of neural network model to predict flow stress for carbon steel, J. Mater. Process. Technol. 141 (2003) 219–227.
[34] S. Srinivasulu, A. Jain, A comparative analysis of training methods for artificial neural network rainfall–runoff models, Appl. Soft Comput. 6 (2006) 295–306.
[35] K. Hornik, M. Stinchcombe, H. White, K. Hornik, M. Stinchcombe, H. White, Multilayer feed forward networks are universal approximators, Neural Networks 2 (5) (1989) 359–366.